Thin Solid Films xxx (2015) xxx–xxx

Contents lists available at ScienceDirect

Thin Solid Films

journal homepage: www.elsevier.com/locate/tsf

Photoelectrochemical properties of orthorhombic and metastable phase SnS nanocrystals synthesized by a facile colloidal method

Po-Chia Huang [a], Jow-Lay Huang [a,b,c], Sheng-Chang Wang [d], Muhammad Omar Shaikh [d], Chia-Yu Lin [e]

[a] Department of Materials Science and Engineering, National Cheng Kung University, Tainan 701, Taiwan, ROC
[b] Department of Chemical and Materials Engineering, National University of Kaohsiung, Kaohsiung 81148, Taiwan, ROC
[c] Center for Micro/Nano Science and Technology, National Cheng Kung University, Tainan 70101, Taiwan, ROC
[d] Department of Mechanical Engineering, Southern Taiwan University of Science and Technology, Tainan 710, Taiwan, ROC
[e] Department of Chemical Engineering, National Cheng Kung University, Tainan 701, Taiwan, ROC

ARTICLE INFO

Article history:
Received 1 April 2015
Received in revised form 3 September 2015
Accepted 7 September 2015
Available online xxxx

Keyword:
Tin sulfur
Orthorhombic
Zinc blende
Metastable phase tin sulfur
Photoelectrochemical cell

ABSTRACT

SnS of orthorhombic (OR) and metastable (SnS) phases were synthesized by using a simple and facile colloidal method. The tin precursor was synthesized using tin oxide (SnO) and oleic acid (OA), while the sulfur precursor was prepared using sulfur powder (S) and oleyamine (OLA). The sulfur precursor was injected into the tin precursor and the prepared SnS nanocrystals were precipitated at a final reaction temperature of 180 °C. The results show that hexamethyldisilazane (HMDS) can be successfully used as a surfactant to synthesize monodisperse 20 nm metastable SnS nanoparticles, while OR phase SnS nanosheets were obtained without HMDS. The direct bandgap observed for the metastable SnS phase is higher (1.66 eV) as compared to the OR phase (1.46 eV). The large blueshift in the direct bandgap of metastable SnS is caused by the difference in crystal structure. The blueshift in the direct band gap value for OR-SnS could be explained by quantum confinement in two dimensions in the very thin nanosheets. SnS thin films used as a photo anode in a photoelectrochemical (PEC) cell were prepared by spin coating on the fluorine-doped tin oxide (FTO) substrates. The photocurrent density of the SnS (metastable SnS)/FTO and SnS (OR)/FTO are 191.8 μA/cm^2 and 57.61 μA/cm^2 at an applied voltage of −1 V at 150 W, respectively. These narrow band gap and low cost nanocrystals can be used for applications in future optoelectronic devices.

1. Introduction

SnS is a p type semiconductor that is being intensely researched worldwide because it has the advantages of being composed of naturally abundant elements and is nontoxic and chemically stable, and thus scaling up its use would be economically and environmentally feasible [1]. It has a high carrier concentration and mobility (hole mobility ~90 cm^2 V^{-1} s^{-1}) [2], a high absorption coefficient (10^4–10^5 cm^{-1} at the fundamental absorption edge, which varies with the phase) [3] and a wide absorption range (band gap ~1.3 eV) [4–8], and thus theoretically possesses all the qualities needed for efficient absorption of solar energy and is suitable for incorporation into photovoltaic cells [9–11], photodetectors [12], photocatalysts [13], field effect transistors [14], Li ion battery anodes [15] and electrochemical capacitors [16,17].

It is well-known that the optoelectronic properties of semiconductor nanocrystals are strongly phase dependent. SnS crystals have been reported in the literature as being in the stable orthorhombic phase or a distorted cubic phase. OR-SnS nanostructures have been synthesized in various forms, including layered nano-crystals [4,5,18], fullerene nanoparticles [19], nanorods [20] and nanobelts [21] by using various techniques, like hydrothermal, solvothermal and pyrolysis methods, among others [4,5,8,22]. In our previous study [23], we controlled different processing parameters to synthesize 20–50 nm SnS nanocrystal thin films with a direct band gap energy of 1.24 eV, while the band gap energy for the sheet-like SnS films was around 1.26 eV.

There has recently been extensive research in synthesizing and characterizing the cubic phase of SnS [7,9,10,14,24–26]. The difference in the crystal structure of this metastable phase as compared to ground state orthorhombic SnS gives rise to novel optoelectronic properties. The metastable phase has a higher band gap of 1.6–1.77 eV as compared to the orthorhombic phase, which has a bandgap of 1.23–1.3 eV. Orthorhombic phase SnS is the thermodynamically stable phase, while the metastable phase SnS is thermodynamically unstable and can be only synthesized under a special artificial environment, like using active surfactants [7,14,26], low reaction temperatures and a short reaction time [9,10,24].

Greyson et al. [24] were the first to synthesize zinc blende (ZB) phase SnS nanoparticles. They observed that when the reaction temperature is lower and the reaction time is short, SnS will change from the orthorhombic to zinc blende phase. The zinc blende phase SnS has a strong absorption edge at around 700 nm (about 1.77 eV). These optical properties are similar to those reported in Deng et al. [7,14] and Avellaneda et al. [9,10]. Deng et al. [14] published a report on synthesizing 2–5 μm long single crystalline ultrathin SnS nanoribbons that

http://dx.doi.org/10.1016/j.tsf.2015.09.081
0040-6090/

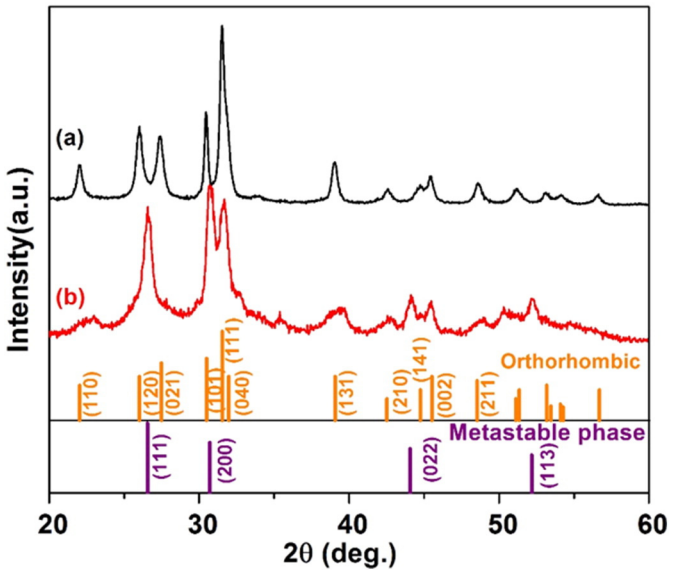

Fig. 1. XRD data for SnS nanocrystals obtained (a) without and (b) with the use of HMDS.

grow via a metastable to stable phase transition, and display dual phase intermediate hetero-structures with ZB nanosphere heads and OR nanoribbon tails.

Metastable phase SnS also tends to exhibit a better direct bandgap and a larger optical absorption range as compared to the stable OR-SnS phase, which could serve to increase SnS performance as a photovoltaic and photoelectrochemical cell material [25]. In the literature, most studies show that metastable SnS has an effective optical absorption onset at around 1.4 eV [27], which is the optimum band gap for achieving maximum efficiency according to the Shockley–Queisser limit under the AM 1.5 solar spectrum. Therefore, metastable SnS could be a more suitable light harvesting material than OR-SnS. Although this metastable SnS phase has been synthesized by many researchers, the crystal structure of this phase is still unclear [25,26], and thus we would like to refer to this phase as metastable SnS. Moreover, the real crystal structure of metastable SnS and its photoelectrical properties remain unknown.

In order to obtain the metastable SnS, suitable surfactants must be used that have a capping effect that prevents the further growth of the metastable SnS to the OR structure. In previous studies, SnS nanoparticles were synthesized using high activity metallic compounds as the tin(II) precursors [5], although these happen to be very toxic. However, nontoxic inorganic SnO is used as the tin source in this study. HMDS has

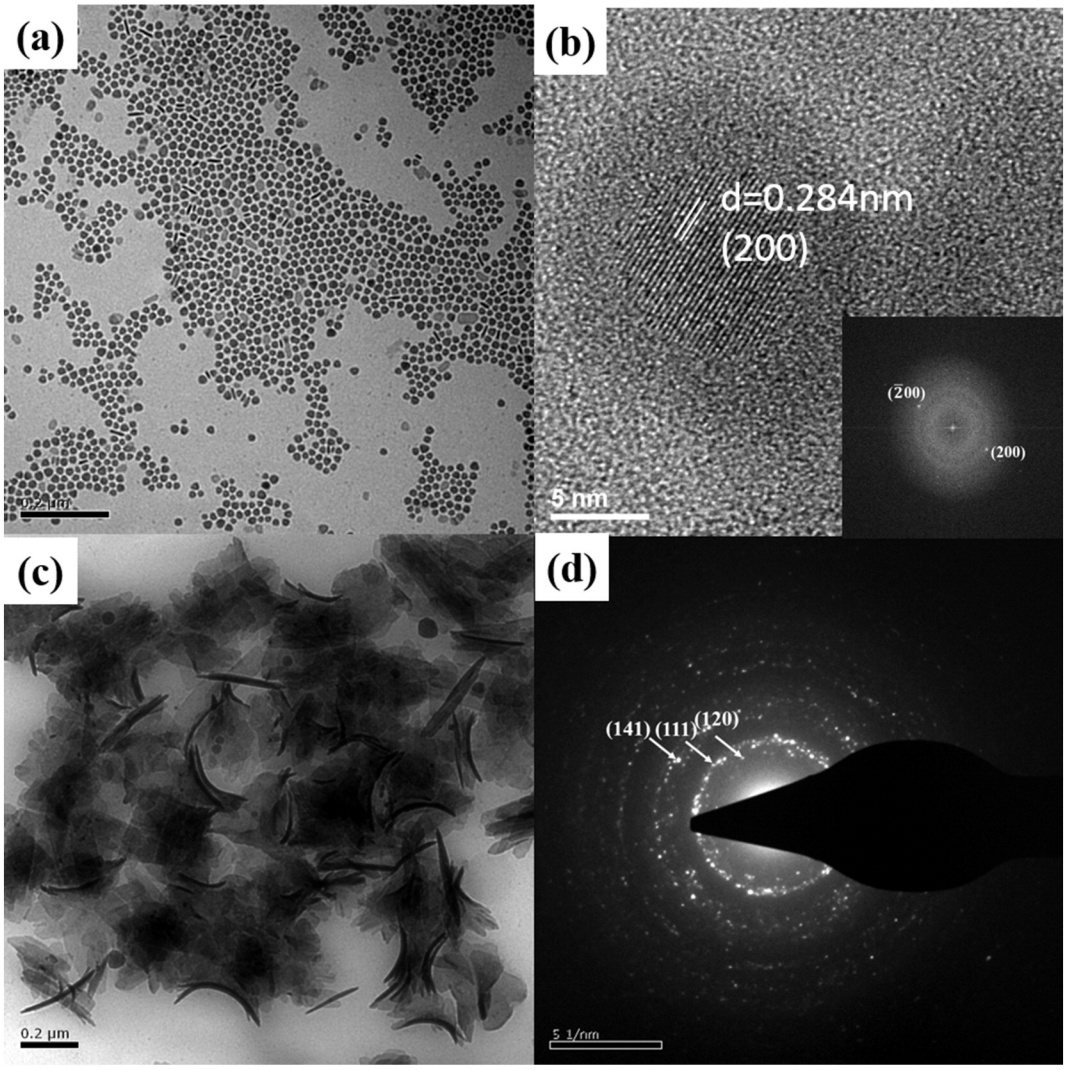

Fig. 2. (a) TEM image showing near monodisperse metastable SnS nanoparticles, (b) HRTEM image showing crystal planes with the inter planar distances used to create indexed FFT patterns (inset), (c) TEM image showing OR-SnS nanosheets obtained without the use of HMDS as a surfactant and (d) SAED diffraction patterns which can be indexed to OR-SnS.

Please cite this article as: P.-C. Huang, et al., Photoelectrochemical properties of orthorhombic and metastable phase SnS nanocrystals synthesized by a facile colloidal method, Thin Solid Films (2015), http://dx.doi.org/10.1016/j.tsf.2015.09.081

been observed to successfully act as a surfactant and capping ligand yielding nearly monodisperse non-agglomerated metastable SnS nanoparticles. To the best of our knowledge, this is the first metastable SnS photoanode for application in a photoelectrochemical cell.

2. Experimental methods

2.1. Synthesis

We used the hot injection method to synthesize metastable SnS nanoparticles with a uniform size distribution, with HMDS (Hexamethyldisilazane, Sigma Aldrich,>99%) as a surfactant to enable colloidal stability and facile surface functionality. In a typical synthesis experiment, 1.35 g of SnO (Tin(II) Oxide, SHOWA, 99%) was mixed with 13.5 ml OA (Oleic Acid, Sigma Aldrich, 66%–88%) and 2 ml of HMDS in a three neck flask and heated to 110 °C under an argon gas inflow with constant magnetic stirring, and held there for 15 min to remove any excess water. It was then heated further to 310 °C, where it became a clear solution forming the tin precursor ($Sn(OA)_X$), after which it was cooled down to 190 °C. Simultaneously, the sulfur precursor (S-OLA) was prepared by heating a mixture of 0.45 mmol of elemental S powder (Sulfur powder, Sigma Aldrich, 98%) and 9 ml OLA (Oleyamine, ACROS, 90%) at 155 °C under magnetic stirring and argon gas inflow. Using glass syringes the hot sulfur precursor was quickly injected into the tin precursor and the final temperature was maintained at 180 °C for 30 min before being cooled to room temperature. All chemicals were used without further purification. The resulting SnS nanoparticle solution was then added to ethanol and acetone in the ratio of 1:9:9, and centrifuged at 5000 rpm for 15 min. This process was repeated several times to wash away all the organic solvents, and the final product was dried in vacuum, re-dispersed in hexane and sent for further characterization. OR-SnS nanosheets were synthesized by the same method, although without the use of HMDS.

Thin films of metastable SnS quantum dots and OR-SnS nanosheets were prepared by spin coating a solution of the obtained nanocrystals (2 mg) in toluene (2 ml) on transparent FTO coated glass substrates. The FTO/glass substrates were subjected to oxygen plasma for 30 s before the spin coating process to aid bonding at the FTO/SnS layer interface. Photo-electrochemical tests were performed in a conventional three electrode system with 0.1 M Na_2SO_4 electrolyte (pH = 7) using the SnS thin films as the working electrode, platinum electrode as the counter electrode and Ag/AgCl as the reference electrode.

2.2. Characterizations

Powder X-Ray diffraction measurements were made on a diffractometer (D2 Phaser, BRUKER, Germany) with Cu Kα radiation (λ = 1.54060 Å) at a scan rate of 0.025° s^{-1} to analyze the phase structure of the nanocrystals. High resolution transmission electron microscopy was performed on a field emission gun transmission electron microscope (Tecnai G2 F20 FEG-TEM, FEI, USA) operating at 200 kV. UV–Vis absorption spectra were obtained using a spectrophotometer equipped with an integrating sphere (JASCO V-650, Japan). The photo-electrochemical properties were measured in ambient conditions under irradiation of a 150 W Xe lamp having a power density of 50 mW cm^{-2}. The potential was swept from 0 to −1.0 V (vs. Ag/AgCl) at a sweep rate of 1 mV/s (PGZ310, Radiometer-analytical, France).

3. Results and discussion

3.1. Structural characterization

Fig. 1(a) is the XRD diffraction peak results, which show the formation of pure OR-SnS without the use of HMDS as a surfactant (JCPDS card no. 39-0354). However when HMDS is used, we observe that the diffraction peaks are purely cubic or orthorhombic, and there is no standard JCPDS that the crystal structure can be assigned to. In the literature metastable phase SnS has been referred to as zinc blende (ZB) [7,9,10,14,24], rock salt (RS) [25] and pseudo-tetragonal [26].

The morphology of the nanocrystals can be seen under bright field TEM (Fig. 2). When HMDS was used as a surfactant, uniformly distributed near-monodisperse nanoparticles were observed with an average particle size of 20 nm. The HRTEM image of the nanoparticles reveals a two dimensional lattice with a typical spacing of 0.284 nm corresponding to (200) of metastable SnS. The indexed fast Fourier transform

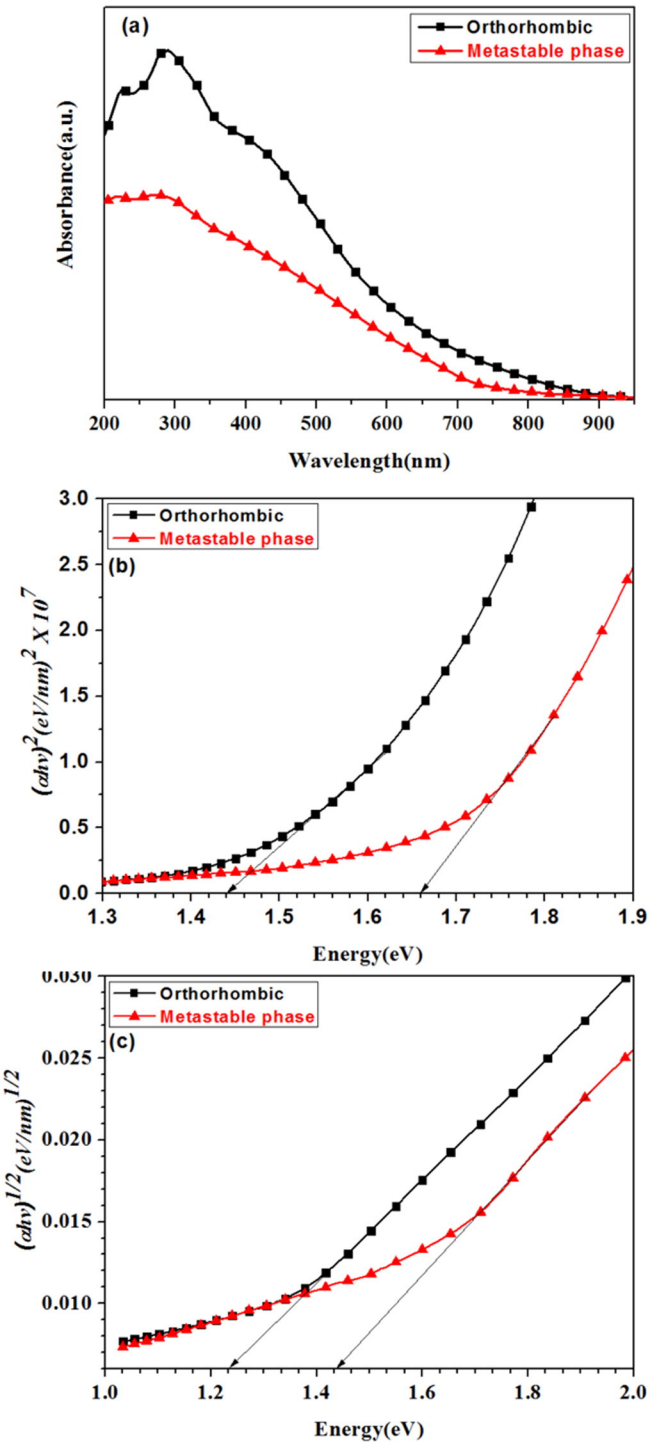

Fig. 3. (a) UV–Vis absorption spectrum as a function of incident photon wavelength. Calculating the bandgap of SnS nanocrystals depending of the type of electronic transition. (b) Direct bandgap, and (c) indirect bandgap.

Please cite this article as: P.-C. Huang, et al., Photoelectrochemical properties of orthorhombic and metastable phase SnS nanocrystals synthesized by a facile colloidal method, Thin Solid Films (2015), http://dx.doi.org/10.1016/j.tsf.2015.09.081

(FFT) of the HRTEM image reveals a pattern that indicates the spherical SnS nanoparticles are single crystals of a metastable phase projected along the (010) direction [26]. Without the use of HMDS, very thin nanosheets that show bending at the edges are observed. The selected area electron diffraction (SAED) pattern shows a polycrystalline structure that can be indexed to the planes of stable OR-SnS.

Here we speculate that adding HMDS may help the tin oleate complex achieve a more suitable balance between the nucleation and growth rates of the metastable phase SnS crystal than is possible with the less reactive tin oleate precursor [7,14]. While fast nucleation occurs, the growth rate of these nucleates is inhibited due to the capping effect of the HMDS (non-nucleophilic base). A vigorous reaction exhibiting bubbling and an immediate color change from clear brown to reddish black is observed when the sulfur precursor is injected into the tin oleate complex. Due to the outburst of energy, the metastable SnS contains a high density of defects and a strained lattice structure, and thus can be synthesized only in a thermodynamically unstable environment. On the other hand, without the use of HMDS, the solution color gradually changes to gray, and no vigorous reaction or bubbling is observed. In the absence of HMDS, the uncapped nucleates can grow into larger nanosheets and crystallize into the stable orthorhombic phase.

3.2. Optical characterization

The optical properties of the nanocrystals were investigated using UV–Vis absorption spectroscopy. The absorption increases at higher photon energies and shows an onset for the OR-SnS phase at about 850 nm, while that of metastable SnS is observed at lower wavelengths of about 750 nm (Fig. 3a).

The optical absorption transitions are used to calculate the band gaps present in the electronic structure of OR-SnS and metastable SnS by performing the Kubelka–Munk transformations [28]. The absorption coefficient is related to the incident photon energy by the formula $(\alpha h\nu)^n = B(h\nu - E_g)$ [29], where a is the absorption coefficient ($\alpha = 2.303\frac{A}{t}$, where t is thickness (3 μm), and A is optical absorbance [30]), $h\nu$ is the incident photon energy, n is a number that depends on the electronic transition and B is a constant. The direct bandgap can be calculated from the x axis intercept in a plot of $(\alpha h\nu)^2$ vs $h\nu$, while the indirect bandgap can be calculated from the x intercept in a plot of $(\alpha h\nu)^{1/2}$ vs $h\nu$.

The values for the direct and indirect bandgap of OR-SnS nanosheets are 1.46 eV and 1.22 eV, respectively, while those for the metastable SnS nanoparticles are 1.66 eV and 1.42 eV respectively (Figs. 3b,c). The strong blueshift (~0.2 eV) for the OR-SnS phase as compared to that reported in the literature (~1.2 eV) could be attributed to quantum confinement effects in the 2-D SnS nanosheets [31]. The higher direct band gap values obtained for metastable SnS agree with the literature (with reports on the previously denoted ZB phase), and are a result of the distortion of the crystal lattice. The difference in optical properties between the two SnS phases can be attributed to their differing lattice parameters (orbital interactions and symmetry of their overlap) and local coordination of atoms. The Bohr exciton radius of SnS quantum dots is in the region of 7 nm [26,32], and thus the larger metastable SnS nanoparticles synthesized in this study would not be strongly affected by quantum confinement effects. The size regime of semiconductor nanoparticles is known to influence the crystalline phase transitions, as observed in the case of metastable SnS, and this can be utilized in creating novel nanoparticles with crystal structures different from their bulk counterparts.

Tailoring reaction conditions to suit the formation of metastable phases and collecting them before they have transformed into their stable phases can enable us to synthesize nanomaterials exhibiting unique optoelectronic properties that can be obtained without utilizing quantum confinement effects.

3.3. Photoelectrochemical characterization

Thin films of SnS nanocrystals used as a working electrode in a PEC cell show relatively high current densities, both in the light and dark at an applied voltage of −1 V vs Ag/AgCl (Figs. 4a,b). The highest photocurrent density observed for metastable SnS is higher (~190 μA/cm^2) than that reported for OR-SnS (~58 μA/cm^2). However notably high current densities are also observed in the dark, and this can be due to the effect of voltage bias on the current flow through the FTO/SnS hetero-junction. While exhibiting near diode characteristics at lower voltages where the charge transport mechanism is tunneling, the charge transport mechanism at higher applied voltages is due to the presence of defects and impurities that affect the space-charge limited current mechanism. The inherent nature of tin vacancy defects in SnS thin films could be the preferred carrier transport mechanism at higher applier voltages, thus showing high current densities even in the dark.

K.R. Gunasekhar et al. [33] observed a high saturation current and diode quality factor at higher bias voltages due to the presence of native defect states. This highlights the low electrical conduction between layers of anisotropic OR-SnS and the more isotropic metastable SnS structure, which results in higher current densities and could thus provide a more suitable thin film absorber material when film thickness in the micrometer range might be needed.

4. Conclusions

In this report we have developed a simple and facile method to synthesize two different phases of SnS having different morphological and optical properties. The use of HMDS as a surfactant resulted in almost spherical near monodisperse metastable SnS nanoparticles, while in its absence thin nanosheets were synthesized that had the stable orthorhombic crystal structure observed in bulk SnS. The blueshift observed in the direct bandgap of OR-SnS and metastable SnS nanocrystals from bulk SnS can be attributed to quantum confinement effects and changes

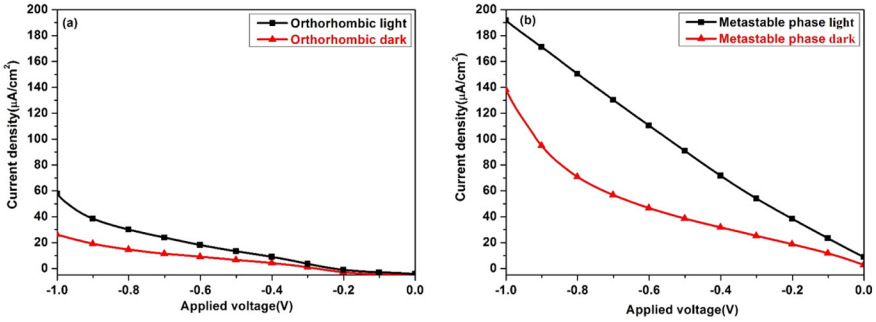

Fig. 4. Current density as a function of the voltage applied between the working electrode and the counter electrode under irradiation of a 150 W Xe lamp having a power density of 50 mW cm^{-2} and in the dark for (a) OR-SnS, and (b) metastable SnS.

Please cite this article as: P.-C. Huang, et al., Photoelectrochemical properties of orthorhombic and metastable phase SnS nanocrystals synthesized by a facile colloidal method, Thin Solid Films (2015), http://dx.doi.org/10.1016/j.tsf.2015.09.081

in the crystal structure, respectively. SnS nanocrystals spin coated on FTO/glass substrates and used as a working electrode in a PEC cell show current densities which increase with applied voltage, and these are higher for the metastable phase. Future research will focus on enhancing the efficiency of SnS as a photo anode by employing earth abundant catalysts.

Acknowledgments

This project was financially supported by the Ministry of Science and Technology of the ROC under contract no. MOST 103-2221-E-218-007 and no. MOST 101-2221-E-006-124-MY3.

References

[1] J.M. Chamberlain, M. Merdan, IR photoconductivity in P-Sns/P-Sns, J. Phys. C Solid State Phys. 10 (1977) L571–L574.
[2] M. Devika, K.T.R. Reddy, N.K. Reddy, K. Ramesh, R. Ganesan, E.S.R. Gopal, K.R. Gunasekhar, Microstructure dependent physical properties of evaporated tin sulfide films, J. Appl. Phys. 100 (2006) 023518–023518-7.
[3] A. Tanusevski, Optical and photoelectric properties of SnS thin films prepared by chemical bath deposition, Semicond. Sci. Technol. 18 (2003) 501–505.
[4] D.S. Koktysh, J.R. McBride, R.D. Geil, B.W. Schmidt, B.R. Rogers, S.J. Rosenthal, Facile route to SnS nanocrystals and their characterization, Mater. Sci. Eng. B 170 (2010) 117–122.
[5] H.T. Liu, Y. Liu, Z. Wang, P. He, Facile synthesis of monodisperse, size-tunable SnS nanoparticles potentially for solar cell energy conversion, Nanotechnology 21 (2010).
[6] J. Liu, D.F. Xue, Sn-based nanomaterials converted from SnS nanobelts: facile synthesis, characterizations, optical properties and energy storage performances, Electrochim. Acta 56 (2010) 243–250.
[7] Z.T. Deng, D.R. Han, Y. Liu, Colloidal synthesis of metastable zinc-blende IV–VI SnS nanocrystals with tunable sizes, Nanoscale 3 (2011) 4346–4351.
[8] P.S. Tang, H.F. Chen, F. Cao, G.X. Pan, K.Y. Wang, M.H. Xu, Y.H. Tong, Nanoparticulate SnS as an efficient photocatalyst under visible-light irradiation, Mater. Lett. 65 (2011) 450–452.
[9] D. Avellaneda, M.T.S. Nair, P.K. Nair, Polymorphic tin sulfide thin films of zinc blende and orthorhombic structures by chemical deposition, J. Electrochem. Soc. 155 (2008) D517–D525.
[10] D. Avellaneda, M.T.S. Nair, P.K. Nair, Photovoltaic structures using chemically deposited tin sulfide thin films, Thin Solid Films 517 (2009) 2500–2502.
[11] Y.F. Sun, Z.H. Sun, S. Gao, H. Cheng, Q.H. Liu, F.C. Lei, S.Q. Wei, Y. Xie, All-surface-atomic-metal chalcogenide sheets for high-efficiency visible-light photoelectrochemical water splitting, Adv. Energy Mater. 4 (2014).
[12] N.K. Reddy, K.T.R. Reddy, Growth of polycrystalline SnS films by spray pyrolysis, Thin Solid Films 325 (1998) 4–6.
[13] J.F. Chao, Z. Xie, X.B. Duan, Y. Dong, Z.R. Wang, J. Xu, B. Liang, B. Shan, J.H. Ye, D. Chen, G.Z. Shen, Visible-light-driven photocatalytic and photoelectrochemical properties of porous SnSx(x = 1,2) architectures, CrystEngComm 14 (2012) 3163–3168.
[14] Z.T. Deng, D. Cao, J. He, S. Lin, S.M. Lindsay, Y. Liu, Solution synthesis of ultrathin single-crystalline SnS nanoribbons for photodetectors via phase transition and surface processing, ACS Nano 6 (2012) 6197–6207.
[15] D.D. Vaughn, O.D. Hentz, S.R. Chen, D.H. Wang, R.E. Schaak, Formation of SnS nanoflowers for lithium ion batteries, Chem. Commun. 48 (2012) 5608–5610.
[16] M. Jayalakshmi, M.M. Rao, B.M. Choudary, Identifying nano SnS as a new electrode material for electrochemical capacitors in aqueous solutions, Electrochem. Commun. 6 (2004) 1119–1122.
[17] J.S. Zhu, D.L. Wang, T.F. Liu, One-pot synthesis of SnS nanorods and their lithium storage properties, Ionics 20 (2014) 141–144.
[18] B.K. Patra, S. Sarkar, A.K. Guria, N. Pradhan, Monodisperse SnS nanocrystals: in just 5 seconds, J. Phys. Chem. Lett. 4 (2013) 3929–3934.
[19] S.Y. Hong, R. Popovitz-Biro, Y. Prior, R. Tenne, Synthesis of SnS2/SnS fullerene-like nanoparticles: a superlattice with polyhedral shape, J. Am. Chem. Soc. 125 (2003) 10470–10474.
[20] H.L. Su, Y. Xie, Y.J. Xiong, P. Gao, Y.T. Qian, Preparation and morphology control of rod-like nanocrystalline tin sulfides via a simple ethanol thermal route, J. Solid State Chem. 161 (2001) 190–196.
[21] C.H. An, K.B. Tang, G.Z. Shen, C.R. Wang, Q. Yang, B. Hai, Y.T. Qian, Growth of belt-like SnS crystals from ethylenediamine solution, J. Cryst. Growth 244 (2002) 333–338.
[22] T. Hyeon, S.S. Lee, J. Park, Y. Chung, H. Bin Na, Synthesis of highly crystalline and monodisperse maghemite nanocrystallites without a size-selection process, J. Am. Chem. Soc. 123 (2001) 12798–12801.
[23] B.Y.J. Liang, Y.M. Shen, S.C. Wang, J.L. Huang, The influence of reaction temperatures and volume of oleic acid to synthesis SnS nanocrystals by using thermal decomposition method, Thin Solid Films 549 (2013) 159–164.
[24] E.C. Greyson, J.E. Barton, T.W. Odom, Tetrahedral zinc blende tin sulfide nano- and microcrystals, Small 2 (2006) 368–371.
[25] L.A. Burton, A. Walsh, Phase stability of the earth-abundant tin sulfides SnS, SnS2, and Sn2S3, J. Phys. Chem. C 116 (2012) 24262–24267.
[26] A.J. Biacchi, D.D. Vaughn, R.E. Schaak, Synthesis and crystallographic analysis of shape-controlled SnS nanocrystal photocatalysts: evidence for a pseudotetragonal structural modification, J. Am. Chem. Soc. 135 (2013) 11634–11644.
[27] W. Shockley, H.J. Queisser, Detailed balance limit of efficiency of P-N junction solar cells, J. Appl. Phys. 32 (1961) 510–519.
[28] P. Geladi, D. Macdougall, H. Martens, Linearization and scatter-correction for near-infrared reflectance spectra of meat, Appl. Spectrosc. 39 (1985) 491–500.
[29] S.Y. Cheng, Y.Q. Chen, C.C. Huang, G.N. Chen, Characterization of SnS films prepared by constant-current electro-deposition, Thin Solid Films 500 (2006) 96–100.
[30] S. Ilican, M. Caglar, Y. Caglar, Determination of the thickness and optical constants of transparent indium-doped ZnO thin films by the envelope method, Mater. Sci. Pol. 25 (2007) 709–718.
[31] S. Sohila, M. Rajalakshmi, C. Ghosh, A.K. Arora, C. Muthamizhchelvan, Optical and raman scattering studies on SnS nanoparticles, J. Alloys Compd. 509 (2011) 5843–5847.
[32] S.G. Hickey, C. Waurisch, B. Rellinghaus, A. Eychmuller, Size and shape control of colloidally synthesized IV–VI nanoparticulate Tin(II) sulfide, J. Am. Chem. Soc. 130 (2008) 14978–14980.
[33] M. Devika, N.K. Reddy, K. Ramesh, F. Patolsky, K.R. Gunasekhar, Weak rectifying behaviour of p-SnS/n-ITO heterojunctions, Solid State Electron. 53 (2009) 630–634.

Please cite this article as: P.-C. Huang, et al., Photoelectrochemical properties of orthorhombic and metastable phase SnS nanocrystals synthesized by a facile colloidal method, Thin Solid Films (2015), http://dx.doi.org/10.1016/j.tsf.2015.09.081